ISSN 1007-9327 (print)
ISSN 2219-2840 (online)

World Journal of *Gastroenterology*

World J Gastroenterol 2018 December 14; 24(46): 5189-5296

Published by Baishideng Publishing Group Inc

World Journal of Gastroenterology

Contents

Weekly Volume 24 Number 46 December 14, 2018

GUIDELINES

MINIREVIEWS

ORIGINAL ARTICLE

Basic Study

Retrospective Study

World Journal of Gastroenterology

Contents

Weekly Volume 24 Number 46 December 14, 2018

Observational Study

Contents

World Journal of Gastroenterology
Volume 24 Number 46 December 14, 2018

ABOUT COVER

Editorial board member of *World Journal of Gastroenterology*, Ilhami Yuksel, MD, Professor, Department of Gastroenterology, Yildirim Beyazit University School of Medicine, Ankara 06100, Turkey

AIMS AND SCOPE

World Journal of Gastroenterology (*World J Gastroenterol*, *WJG*, print ISSN 1007-9327, online ISSN 2219-2840, DOI: 10.3748) is a peer-reviewed open access journal. *WJG* was established on October 1, 1995. It is published weekly on the 7th, 14th, 21st, and 28th each month. The *WJG* Editorial Board consists of 642 experts in gastroenterology and hepatology from 59 countries.

The primary task of *WJG* is to rapidly publish high-quality original articles, reviews, and commentaries in the fields of gastroenterology, hepatology, gastrointestinal endoscopy, gastrointestinal surgery, hepatobiliary surgery, gastrointestinal oncology, gastrointestinal radiation oncology, gastrointestinal imaging, gastrointestinal interventional therapy, gastrointestinal infectious diseases, gastrointestinal pharmacology, gastrointestinal pathophysiology, gastrointestinal pathology, evidence-based medicine in gastroenterology, pancreatology, gastrointestinal laboratory medicine, gastrointestinal molecular biology, gastrointestinal immunology, gastrointestinal microbiology, gastrointestinal genetics, gastrointestinal translational medicine, gastrointestinal diagnostics, and gastrointestinal therapeutics. *WJG* is dedicated to become an influential and prestigious journal in gastroenterology and hepatology, to promote the development of above disciplines, and to improve the diagnostic and therapeutic skill and expertise of clinicians.

INDEXING/ABSTRACTING

World Journal of Gastroenterology (*WJG*) is now indexed in Current Contents®/Clinical Medicine, Science Citation Index Expanded (also known as SciSearch®), Journal Citation Reports®, Index Medicus, MEDLINE, PubMed, PubMed Central and Directory of Open Access Journals. The 2018 edition of Journal Citation Reports® cites the 2017 impact factor for *WJG* as 3.300 (5-year impact factor: 3.387), ranking *WJG* as 35th among 80 journals in gastroenterology and hepatology (quartile in category Q2).

NAME OF JOURNAL
World Journal of Gastroenterology

ISSN
ISSN 1007-9327 (print)
ISSN 2219-2840 (online)

LAUNCH DATE
October 1, 1995

FREQUENCY
Weekly

EDITORIAL OFFICE
Ze-Mao Gong, Director
World Journal of Gastroenterology
Baishideng Publishing Group Inc
7901 Stoneridge Drive, Suite 501,
Pleasanton, CA 94588, USA
Telephone: +1-925-2238242
Fax: +1-925-2238243
E-mail: editorialoffice@wjgnet.com
Help Desk: https://www.f6publishing.com/helpdesk
https://www.wjgnet.com

PUBLISHER
Baishideng Publishing Group Inc
7901 Stoneridge Drive, Suite 501,
Pleasanton, CA 94588, USA
Telephone: +1-925-2238242
Fax: +1-925-2238243
E-mail: bpgoffice@wjgnet.com
Help Desk: https://www.f6publishing.com/helpdesk
https://www.wjgnet.com

PUBLICATION DATE
December 14, 2018

INSTRUCTIONS TO AUTHORS
Full instructions are available online at https://www.wjgnet.com/bpg/gerinfo/204

ONLINE SUBMISSION
https://www.f6publishing.com

World Journal of Gastroenterology

Submit a Manuscript: https://www.f6publishing.com

World J Gastroenterol 2018 December 14; 24(46): 5246-5258

DOI: 10.3748/wjg.v24.i46.5246

ISSN 1007-9327 (print) ISSN 2219-2840 (online)

ORIGINAL ARTICLE

Basic Study

Effect of photodynamic therapy with (17R,18R)-2-(1-hexyloxyethyl)-2-devinyl chlorine E6 trisodium salt on pancreatic cancer cells *in vitro* and *in vivo*

Yu-Jie Shen, Jia Cao, Fang Sun, Xiao-Lei Cai, Ming-Ming Li, Nan-Nan Zheng, Chun-Ying Qu, Yi Zhang, Feng Shen, Min Zhou, Ying-Wei Chen, Lei-Ming Xu

Yu-Jie Shen, Jia Cao, Fang Sun, Xiao-Lei Cai, Ming-Ming Li, Nan-Nan Zheng, Chun-Ying Qu, Yi Zhang, Feng Shen, Min Zhou, Ying-Wei Chen, Lei-Ming Xu, Department of Gastroenterology, Xinhua Hospital Affiliated to Shanghai Jiao Tong University School of Medicine, Shanghai 200092, China

ORCID number: Yu-Jie Shen (0000-0002-8517-379X); Jia Cao (0000-0002-6298-3685); Fang Sun (0000-0002-6688-4676); Xiao-Lei Cai (0000-0001-6961-2935); Ming-Ming Li (0000-0001-5181-4125); Nan-Nan Zheng (0000-0002-5628-406X); Chun-Ying Qu (0000-0003-1846-1924); Yi Zhang (0000-0002-1363-3291); Feng Shen (0000-0001-7782-2211); Min Zhou (0000-0002-5371-1098); Ying-Wei Chen (0000-0002-5163-9555); Lei-Ming Xu (0000-0002-6735-4853).

Author contributions: Shen YJ and Cao J contributed equally to this work. Shen YJ and Cao J performed the majority of the experiments and wrote the paper; Sun F, Cai XL, Li MM, and Zheng NN analyzed the data; Qu CY, Zhang Y, Shen F, Zhou M, and Chen YW edited the manuscript; Xu LM designed and supervised the study; All authors have read and agreed with the final manuscript.

Supported by National Natural Science Foundation of China, No. 81472844.

Institutional review board statement: This study was reviewed and approved by the Ethics Committee of Xinhua Hospital Affiliated to Shanghai Jiao Tong University School of Medicine (XHEC-NSFC-2018-036).

Institutional animal care and use committee statement: This study was reviewed and approved by the Ethics Committee of Xinhua Hospital Affiliated to Shanghai Jiao Tong University School of Medicine (XHEC-F-NSFC-2018-016).

Conflict-of-interest statement: The authors declare that there are no conflicts of interest related to this study.

Data sharing statement: No additional data are available.

ARRIVE guidelines statement: The ARRIVE guidelines have been adopted.

Manuscript source: Unsolicited manuscript

Corresponding author to: Lei-Ming Xu, MD, PhD, Chief Doctor, Chief Physician, Department of Gastroenterology, Xinhua Hospital Affiliated to Shanghai Jiao Tong University School of Medicine, 1665 Kongjiang Road, Yangpu District, Shanghai 200092, China. xuleiming@xinhuamed.com.cn
Telephone: +86-21-25078999
Fax: +86-21-25078999

Received: September 25, 2018
Peer-review started: September 25, 2018
First decision: October 16, 2018
Revised: October 28, 2018
Accepted: November 13, 2018
Article in press: November 13, 2018
Published online: December 14, 2018

Abstract

AIM

To investigate the antitumor effects and underlying mechanisms of (17R,18R)-2-(1-hexyloxyethyl)-2-devinyl chlorine E6 trisodium salt (YLG-1)-induced photodynamic therapy (PDT) on pancreatic cancer *in vitro* and *in vivo*.

METHODS
YLG-1 is a novel photosensitizer extracted from spirulina. Its phototoxicity, cellular uptake and localization, as well as its effect on reactive oxygen species (ROS) production, apoptosis, and expression of apoptosis-associated proteins were detected *in vitro*. An *in vivo* imaging system (IVIS), the Lumina K imaging system, and mouse models of subcutaneous Panc-1-bearing tumors were exploited to evaluate the drug delivery pathway and pancreatic cancer growth *in vivo*.

RESULTS
YLG-1 was localized to the mitochondria, and the appropriate incubation time was 6 h. Under 650 nm light irradiation, YLG-1-PDT exerted a potent cytotoxic effect on pancreatic cancer cells *in vitro*, which could be abolished by the ROS scavenger N-acetyl-L-cysteine (NAC). The death mode caused by YLG-1-PDT was apoptosis, accompanied by upregulated Bax and cleaved Caspase-3 and decreased Bcl-2 expression. The results from the IVIS images suggested that the optimal administration route was intratumoral (IT) injection and that the best time to conduct YLG-1-PDT was 2 h post-IT injection. Consistent with the results *in vitro*, YLG-1-PDT showed great growth inhibition effects on pancreatic cancer cells in a mouse model.

CONCLUSION
YLG-1 is a potential photosensitizer for pancreatic cancer PDT *via* IT injection, the mechanisms of which are associated with inducing ROS and promoting apoptosis.

Key words: Photodynamic therapy; Pancreatic neoplasm; (17R,18R)-2-(1-hexyloxyethyl)-2-devinyl chlorine E6 trisodium salt; Antitumor effect

Core tip: Photodynamic therapy (PDT) has become a feasible treatment for advanced pancreatic neoplasms. Photosensitizers play a critical role in PDT. (17R,18R)-2-(1-hexyloxyethyl)-2-devinyl chlorine E6 trisodium salt (YLG-1) is a promising photosensitizer with high water solubility and phototoxicity. The functions of YLG-1-induced PDT (YLG-1-PDT) are still poorly understood. We found that YLG-1-PDT displayed great antitumor effects on pancreatic cancer cells *in vitro* and *in vivo*, the mechanisms of which involved inducing reactive oxygen species and promoting apoptosis. The optimal administration of YLG-1 towards pancreatic cancer is an intratumoral injection. Our study suggests that YLG-1 is a potential photosensitizer for pancreatic neoplasm PDT.

Shen YJ, Cao J, Sun F, Cai XL, Li MM, Zheng NN, Qu CY, Zhang Y, Shen F, Zhou M, Chen YW, Xu LM. Effect of photodynamic therapy with (17R,18R)-2-(1-hexyloxyethyl)-2-devinyl chlorine E6 trisodium salt on pancreatic cancer cells *in vitro* and *in vivo*. *World J Gastroenterol* 2018; 24(46): 5246-5258
URL: https://www.wjgnet.com/1007-9327/full/v24/i46/5246.htm
DOI: https://dx.doi.org/10.3748/wjg.v24.i46.5246

INTRODUCTION

Pancreatic cancer is one of the most malignant diseases, with a 5-year survival rate less than 5%[1]. Despite advancements in therapies, the overall prognosis remains dismal. Local invasion, early metastasis, and tumor cell chemoresistance after radical surgery or various treatments account for the low survival rate[2]. Therefore, there is still a great need for additional therapies to improve the prognosis of pancreatic cancer.

Photodynamic therapy (PDT) is a minimally invasive ablation of local tumors and other diseases that impairs target cells or microorganisms *via* inducing the production of reactive oxygen species (ROS)[3,4]. Photosensitizer accumulation in target tissues, specific light wavelengths, and oxygen are at the core of PDT[5]. A growing body of studies indicate that PDT is a promising therapy for tumors in that it not only directly kills tumor cells and damages the tumor vasculature but also enhances antitumor immune responses to prevent recurrence[6,7]. However, the characteristics associated with pancreatic cancer, including its deep location and hypovascular nature, seriously affect optical accessibility and photosensitizer accumulation in tumor tissues, which limits the application of PDT in pancreatic cancer therapy. With the development of endoscopic ultrasonography (EUS) and EUS-guided fine needle aspiration (EUS-FNA), the problems associated with optical accessibility have been well resolved. Initially, EUS and EUS-FNA have been applied in pancreatic neoplasm diagnosis. In 2015, Choi *et al*[8] demonstrated that EUS-guided PDT with a flexible laser-light catheter inserted directly into the tumor is feasible and safe for locally advanced pancreaticobiliary malignancies. Thus, the selection of an appropriate photosensitizer is currently of critical importance for PDT.

Chlorins are second-generation photosensitizers with a longer absorption band (650 nm), more ROS generation, and lower skin sensitivity than commercially available porphyrin photosensitizers (630 nm) such as 5-aminolevulinic acid (5-ALA) and porfimer sodium (Photofrin)[5,9,10]. (17R,18R)-2-(1-hexyloxyethyl)-2-devinyl chlorine E6 trisodium salt (YLG-1) is a hydrophilic chlorine derivative extracted from spirulina chlorophyll. Spirulina is now being considered as a health supplement but has a light sensitivity as a side effect[11]. It has been used as the raw material for many photosensitizers including methyl 3-[1'-(m-iodobenzyloxy) ethyl] pyropheophorbide-a 2, selenium-containing phycocyanin, and chlorin e6 (Ce6)[12-14]. YLG-1 was initially approved as a disinfection product owing to its great antimicrobial effect under PDT. It possesses various characteristics including a high purity of 99.5%, high water-solubility, high chemical stability, high phototoxicity, low dark toxicity, and a low price according to the product manual. The advantages of YLG-1 make it a potential candidate for applications in

clinical work. However, the functions of YLG-1-induced PDT (YLG-1-PDT) are still poorly understood, with no available publications. Thus, we wondered whether YLG-1-PDT displays antitumor efficacy.

Here, we evaluated the antitumor effects and associated mechanisms of YLG-1-PDT on pancreatic cancer cells *in vitro* and *in vivo*. YLG-1 was found to be localized to the mitochondria and exert great phototoxicity on pancreatic cancer cells *in vitro*, the mechanisms of which involved inducing ROS production and apoptosis. To ensure the photosensitizer to accumulate in pancreatic tumors *in vivo*, YLG-1 was administered by intratumoral (IT) injection according to *in vivo* imaging system (IVIS) images. In *in vivo* experiments, pancreatic tumor growth was potently inhibited by YLG-1-PDT. We thus proposed that YLG-1 is a potential photosensitizer in pancreatic cancer PDT. Our findings provided fundamental research for the clinical application of YLG-1 in pancreatic cancer therapies.

MATERIALS AND METHODS

Materials and light source

YLG-1 was provided by Guilin Huiang Biochemistry Pharmaceutical Co., Ltd (Guilin, China). It was dissolved in phosphate buffer solution (PBS; Solarbio, China) to obtain a 10 mg/mL solution and then stored at 4 ℃. The 650-nm laser PDT instrument was provided by Guilin Xingda Photoelectric Medical Equipment Co., Ltd (Guilin, China).

Absorption and emission spectra

The UV-Vis absorption spectrum of YLG-1 was measured on an ultraviolet visible spectrophotometer (UV-2550, Shimadzu, Kyoto, Japan). The fluorescence (FL) spectra were detected using a fluorescence spectrometer (LS-55, PerkinElmer, Waltham, MA, United States). Slits were kept narrow to 1 nm for excitation and at 1 or 2 nm for emission.

Cell culture

The human pancreatic cancer cell lines SW1990 and Panc-1 were purchased from the cell bank of the Type Culture Collection of the Chinese Academy of Sciences (Shanghai, China). SW1990 and Panc-1 cells were cultured in RPMI 1640 medium (GIBCO, Grand Island, NY, United States) or DMEM (GIBCO), respectively, with 10% fetal bovine serum (FBS) (GIBCO) at 37 ℃ in a 5% CO_2 atmosphere.

Intracellular uptake and localization of YLG-1

SW1990 or Panc-1 cells were seeded in 12-well plates and cultured to 70%-80% confluence. The cells were treated with serum-free culture medium containing 0.5 μg/mL YLG-1 at 37 ℃ for 0-12 h. After washing twice with PBS, the cells were treated with 500 μL cell lysate (0.3% Triton X-100 in PBS) for 30 min at 37 ℃ as described in a previous report[15]. Then, the cell lysate was centrifuged to acquire the supernatant. The FL intensity of 100 μL supernatant was determined using a Bio-Tek Synergy H1 (Ex = 397 nm and Em = 652 nm) (Bio-Tek, Winooski, VT, United States).

To locate the YLG-1, the cells were cultured to 40%-60% confluence, loaded with 0.5 μg/mL YLG-1 for 6 h in serum-free culture medium, and then incubated with 100 nmol/L MitoTracker Green FM (Yeasen Biotechnology, Shanghai, China) (Ex = 490 nm and Em = 516 nm) for 30 min to label mitochondria. The cells were then washed with PBS and replaced with fresh culture medium. Then, a confocal microscope (Leica, Wetzlar, Germany) was used to observe the FL.

Phototoxicity of YLG-1-PDT in vitro

Cells were incubated with YLG-1 at concentrations ranging from 0 to 5 μg/mL in serum-free culture at 37 ℃ or exposed to laser light doses of 0 to 10 J/cm^2 at 650 nm. After 24 h, the cells were subjected to CCK-8 assay (Yeasen Biotechnology) according to the manufacturer's protocol. The absorbance was measured at 450 nm with the Bio-Tek Synergy H1. In another experiment, the cells were incubated with the indicated dose of YLG-1 for an indicated time and then irradiated at 5 or 10 J/cm^2 for CCK-8 assay after 24 h.

Intracellular ROS production

Cells were incubated with the indicated dose of YLG-1 for 6 h with or without exposure to laser light (10 J/cm^2) and then divided into the following four groups: control (Con) group, light-only (Light) group, YLG-1 alone (YLG-1) group, and YLG-1-PDT (PDT) group. Before irradiation, the cells were incubated with 10 μmol/L DCFH-DA (ROS-sensitive probe; Yeasen Biotechnology) for 30 min at 37 ℃. The intracellular ROS was detected by observing the DCF using the Leica DMI6000B Live Cell Application (Leica, Wetzlar, Germany) at 1 h postirradiation. To quantitatively detect the FL intensity of the DCF, the cells were treated with 0.3% Triton X-100 for 30 min at 37 ℃ and centrifuged to acquire the supernatant. The FL intensity was read with the Bio-Tek Synergy H1 (Ex = 488 nm and Em = 525 nm). In another experiment, the PDT group was preincubated with 5 mmol/L N-acetyl-L-cysteine (NAC) (Yeasen Biotechnology), an ROS scavenger, for 1 h before irradiation. The following steps were conducted as mentioned above. Cell viability was evaluated using the CCK-8 assay.

Apoptosis analysis in vitro

Cell grouping and culturing conditions were consistent with the aforementioned experiments. At 4 h after illumination, the cells were harvested for staining with Alexa Fluor 488 Annexin V and propidium iodide (PI) (BD apoptosis assay kit, BD Pharmingen, CA, United States) according to the manufacturer's protocol. In total, 10^4 cells per group were analyzed immediately using a FACSCalibur flow cytometer (BD Biosciences, CA, United States). The data were analyzed using the FlowJo

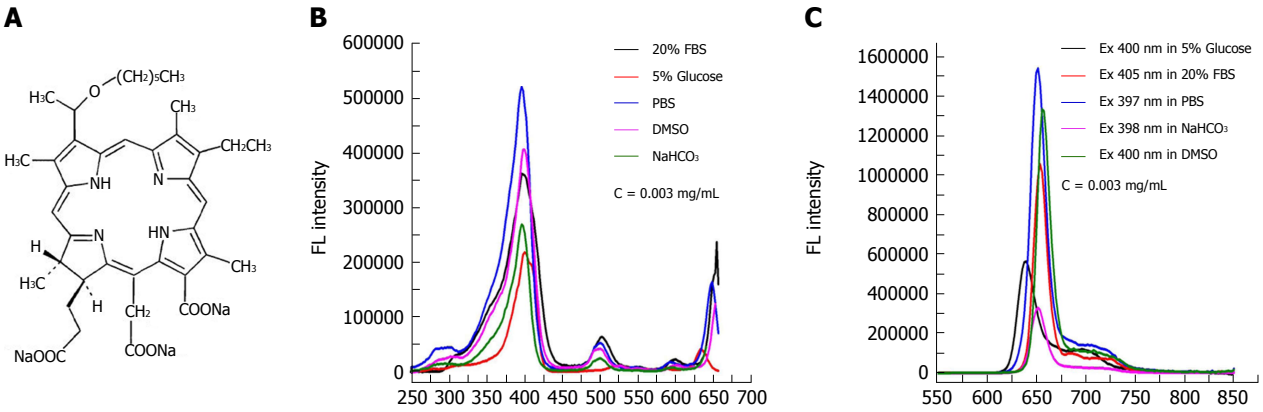

Figure 1 Chemical structure and spectral properties of (17R,18R)-2-(1-hexyloxyethyl)-2-devinyl chlorine E6 trisodium salt. A: Chemical structure of the photosensitizer (17R,18R)-2-(1-hexyloxyethyl)-2-devinyl chlorine E6 trisodium salt (YLG-1). B: Absorption spectra of YLG-1 in different solutions. C: Fluorescence emission spectra of YLG-1 in different solutions excited at different wavelengths. FL: Fluorescence; YLG-1: (17R,18R)-2-(1-hexyloxyethyl)-2-devinyl chlorine E6 trisodium salt.

software.

Western blot

To detect apoptosis-associated protein expression, cells were collected for Western blot assay at 8 h after illumination. In total, 20-40 μg protein/well was separated on 10% or 12% SDS-polyacrylamide gels and transferred to PVDF membranes. After blocking with 5% BSA (Yeasen Biotechnology), the blots were incubated with antibodies (Cell Signaling Technology, Danvers, United States) against β-actin (1:3000), Bax (1:1000), Bcl-2 (1:1000), and Caspase-3 (1:1000) overnight at 4 ℃. The membranes were subjected to incubation with HRP-conjugated secondary antibodies (Yeasen Biotechnology) for 1 h. Finally, the proteins were detected using enhanced chemiluminescent reagents (Yeasen Biotechnology).

Detecting the biodistribution of YLG-1 in vivo

Female BALB/c nude mice at 6 wk of age were purchased from the Shanghai Laboratory Animal Center of the Chinese Academy of Sciences and reared in a specific pathogen-free facility (23 ℃, 12 h/12 h light/dark cycle, 50% humidity, and *ad libitum* access to food and water). All experimental procedures were approved by the ethics committee of Xinhua Hospital Affiliated to Shanghai Jiao Tong University School of Medicine, with approved institutional protocols set by the China Association of Laboratory Animal Care. Panc-1 cells (5×10^6) suspended in 100 μL cold PBS were subcutaneously injected into the lower back region of mice. The tumor volume was calculated using the following formula: $1/2 \times \text{width}^2 \times \text{length}$. When tumors sizes reached approximately 100 mm^3, the surviving mice were intraperitoneally injected with 60, 30, or 8 mg/kg YLG-1 or intratumorally with YLG-1 at doses of 30 or 8 mg/kg. At the indicated time points, the mice were intraperitoneally anesthetized with 10 mg/mL pentobarbital sodium (40 mg/kg) for imaging using an IVIS Lumina K Series Ⅲ imaging system (PerkinElmer, United States) (Ex = 420 nm and Em = 670 nm; the optimal absorbance and emission peaks were unavailable using this IVIS imaging system). The FL intensity of YLG-1 in the tumor site was quantified under the same color scale (min = $6.35e^8$ and max = $6.31e^9$).

Antitumor effects of YLG-1-PDT in vivo

The Panc-1 tumor-bearing mice were randomly divided into the following four groups (n = 6) when the tumors volumes reached 100 mm^3: Con group, Light group, YLG-1 group, and PDT group. Mice in the PDT group were intratumorally injected with 8 mg/kg YLG-1 followed by 650 nm laser-irradiation (100 J/cm^2) at 2 h postinjection. The Light and YLG-1 groups received the same intensity of irradiation or the same dosage of YLG-1 as the PDT group. The subcutaneous tumors were measured within 14 d. Tumor tissue was embedded and sliced for staining with hematoxylin and eosin (H&E). Histopathological changes were observed under a light microscope (DMI4000 B, Leica Microsystems, Wetzlar, Germany). No body weight changes or other apparent adverse effects were observed on the mice during the study period.

Statistical analysis

All data are shown as the mean ± SD and replicated three or more times. All data were assessed by t-tests and one-way ANOVA (SPSS 17.0 software). P values < 0.05 were considered statistically significant.

RESULTS

Chemical structure and spectral properties of YLG-1

The chemical structure of the photosensitizer YLG-1 is shown in Figure 1A. YLG-1 dissolved in different solutions had similar spectral peak positions but at different values, suggesting the high chemical stability of YLG-1. It appeared that PBS was the optimal solution for YLG, with strong absorption and emission peaks (Figure 1B and C). In our study, YLG-1 was dissolved in PBS, which had several distinct absorption peaks at approximately 397 nm, 500 nm, 600 nm, and 652 nm; the maximum

peak was at 397 nm. As shown in Figure 1C, the peak emission for FL was detected at approximately 652 nm. Considering the penetration depth of light, 650 nm laser irradiation was used in the PDT for pancreatic cancer.

Phototoxicity, cellular uptake, and subcellular localization of YLG-1 in vitro

As shown in Figure 2A and B, YLG-1 (0-5 μg/mL) or light (0-10 J/cm^2) alone had no significant cytotoxicity on the cells at 24 h posttreatment. To assess the appropriate incubation time for YLG-1 with cells, the cells were incubated with 0.5 μg/mL YLG-1 for 0-12 h. The YLG-1 FL intensity increased with time and peaked at 6 h in SW1990 and Panc-1 cells, before fading with time during the next 6-12 h (Figure 2C). Therefore, 6 h was selected as the incubation time in the following experiments.

Next, we investigated the subcellular localization of YLG-1 using mitochondrial FL probes. The cells were loaded with 0.5 μg/mL YLG-1 for 6 h and incubated with MitoTracker Green FM for 30 min. Yellow FL regions showed overlap between the mitochondria (green FL) and YLG-1 (red FL). The results showed that YLG-1 was primarily localized in mitochondria (Figure 2D).

To study the influence of YLG-1-PDT on cell viability, SW1990 or Panc-1 cells were incubated with 0-0.25 or 0-1 μg/mL YLG-1 for 6 h, respectively. As shown in Figure 2E, enhanced cell death occurred with higher YLG-1 concentrations and illumination doses. Cell viability was significantly decreased by YLG-1-PDT in SW1990 cells (IC_{50} = 0.18 μg/mL at 5 J/cm^2 and 0.13 μg/ml at 10 J/cm^2) and Panc-1 (IC_{50} = 0.67 μg/mL at 5 J/cm^2 and 0.46 μg/mL at 10 J/cm^2). Hence, 0.13 and 0.46 μg/mL YLG-1 at a light intensity of 10 J/cm^2 was used in the following ROS production and apoptosis experiments.

ROS production triggered by YLG-1-PDT in vitro

To understand the therapeutic mechanisms of YLG-1-PDT in killing pancreatic cancer, we detected cellular ROS production and the frequency of apoptosis *in vitro*. As shown in Figure 3A and B, ROS generation increased significantly in both the SW1990 and Panc-1 cell PDT groups (0.13 and 0.46 μg/mL, respectively, and 10 J/cm^2) at 1 h postirradiation compared with the Con groups, while no significant changes in ROS contents were observed among the YLG-1, Light, and Con groups. To verify the role of ROS in YLG-1-PDT-induced cytotoxicity, we pretreated cells with ROS scavenger (5 mmol/L NAC) 1 h prior to irradiation. When ROS production was inhibited by NAC, pancreatic cancer cell viability was also restored (Figure 3C). These data indicated that YLG-1-PDT could kill pancreatic cancer cells by inducing the production of ROS.

Apoptosis and apoptosis-associated protein expression induced by YLG-1-PDT

To investigate the cell death mechanism of pancreatic cancer cells induced by YLG-1-PDT, flow cytometry was performed 4 h after treatment. As shown in Figure 4A, the rates of early and late apoptosis were dramatically higher in the SW1990 and Panc-1 cell PDT groups than in the Con groups (44.03% in the SW1990 PDT group *vs* 10.09% in the Con group and 29.2% in the Panc-1 PDT group *vs* 2.35% in the Con group, respectively), while those in the YLG-1, Light, and Con groups exhibited no significant changes. Moreover, the pro-apoptotic protein expression of Bax and cleaved Caspase-3 in both the SW1990 and Panc-1 PDT groups was significantly upregulated compared to the Con groups at 8 h postillumination, while anti-apoptotic Bcl-2 expression showed the opposite results (Figure 4B). Meanwhile, the YLG-1 and Light groups showed no obvious alterations in the expression of those proteins compared to the Con groups. Therefore, YLG-1-PDT promoted pancreatic tumor apoptosis by upregulating cleaved Caspase-3 and Bax expression and downregulating Bcl-2 expression.

Biodistribution and accumulation of YLG-1 in vivo

To select the appropriate YLG-1 administration route, we detected the biodistribution of YLG-1 *via* intraperitoneal (IP) and IT injection in Panc-1 tumor-bearing mice using an IVIS Lumina K imaging system. As displayed in Figure 5A, the mice listed from left to right were respectively administered with 60, 30, and 8 mg/kg YLG-1 *via* IP injection and 8 mg/kg YLG-1 by IT injection. IVIS images were captured at 5, 24, and 48 h postinjection. The images showed that the FL of YLG-1 was widely distributed throughout the mouse bodies 5 h after IP injection with three doses of YLG and did not show tumor-specific accumulation. In contrast, mice treated with YLG-1 IT injections showed strong FL signals concentrated in the tumor with weak signals in other parts of the body. Later, the YLG-1 FL signal in all the mice faded away. The FL signal in the mice with IT injections declined at a considerably slower rate compared with mice with IP injections. We believe that the low tumor-specific accumulation of YLG-1 by systemic administration was due to the rapid clearance of free small molecular compounds from the blood circulation. Thus, our data suggested the optimal drug delivery route for YLG-1 was IT injection.

As shown in Figure 5B, when the IT injection dosage of YLG-1 reached 30 mg/kg YLG-1, FL signal in the tumor area appeared oversaturated and the outline of the tumor could not be clearly depicted. This phenomenon indicated that YLG-1 overflowed into the surrounding region, which might damage the surrounding tissues and result in some complications when conducting PDT.

To better evaluate the FL biodistribution of YLG-1 at various time points, the tumor-bearing mice were intratumorally injected with 8 mg/kg YLG-1 and imaged at 0-4 h postinjection. The FL signal in the tumor could be clearly detected at 1 h after injection and rapidly peaked at 2 h (Figure 5C). Then, the average FL intensity declined, decreasing to approximately 50% at 4 h postinjection (from $5.46 \times 10^9 \pm 1.414 \times 10^8$ to $2.45 \times 10^9 \pm 1.56 \times 10^8$). Therefore, we determined that the best time

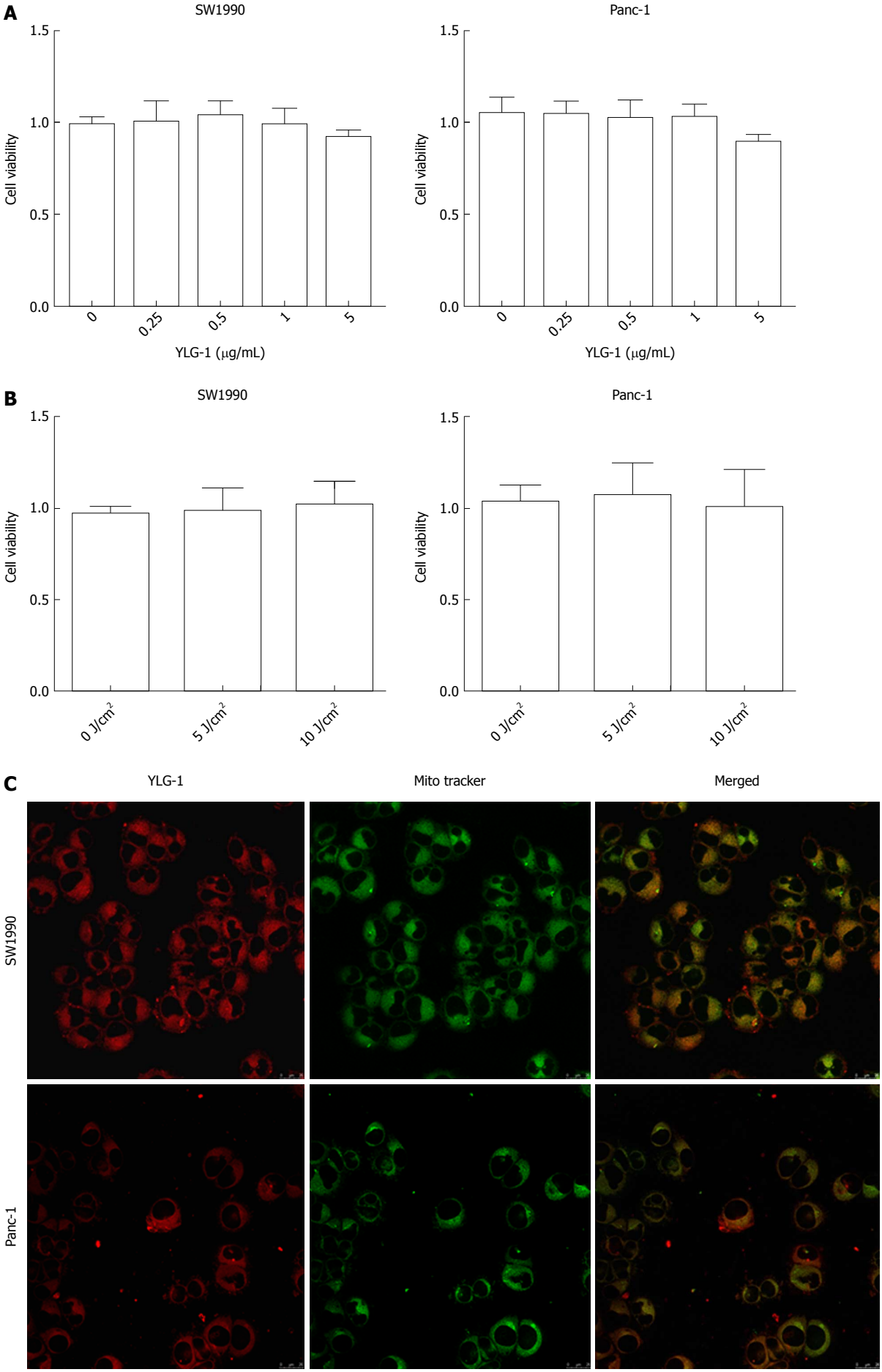
A
SW1990
Panc-1
Cell viability
1.5
1.0
0.5
0.0
0
0.25
0.5
1
5
YLG-1 (μg/mL)
B
SW1990
Panc-1
Cell viability
0 J/cm2
5 J/cm2
10 J/cm2
C
YLG-1
Mito tracker
Merged
SW1990
Panc-1

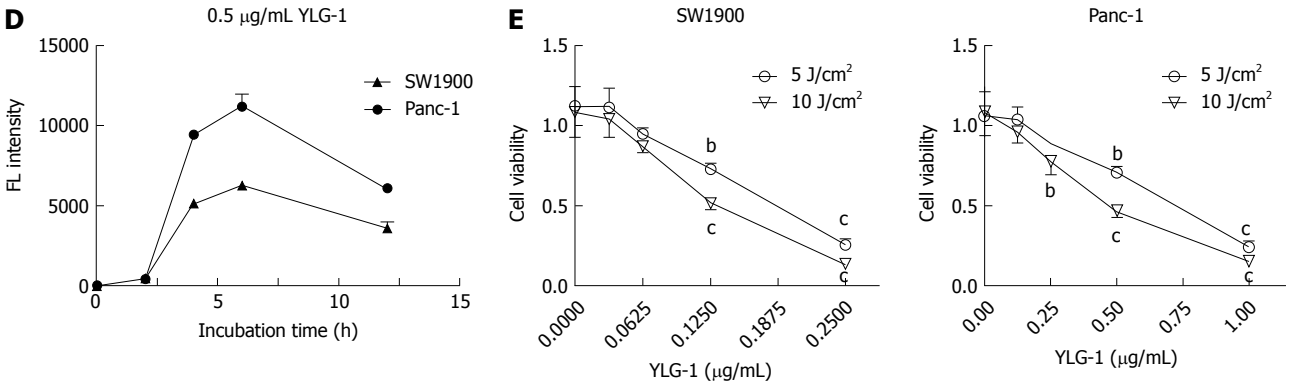

Figure 2 Phototoxicity, cellular uptake, and localization of (17R,18R)-2-(1-hexyloxyethyl)-2-devinyl chlorine E6 trisodium salt *in vitro*. A: Effect of various concentrations of (17R,18R)-2-(1-hexyloxyethyl)-2-devinyl chlorine E6 trisodium salt (YLG-1) (0-5 μg/mL) alone on SW1990 and Panc-1 cell viability. B: Influence of different doses of laser light (0-10 J/cm^2) on pancreatic cancer cell viability. C: Intracellular localization of YLG-1. Red, green, and yellow fluorescence (FL) corresponded to YLG-1, MitoTracker-stained mitochondria, and colocalization of the red and green FL, respectively. Scale bar = 25 μm. D: Cellular uptake of YLG-1 detected at 0-12 h *via* incubation with 0.5 μg/mL YLG-1 in vitro. E: SW1990 and Panc-1 cells incubated with 0-0.25 or 0-1.0 μg/mL YLG-1 for 6 h followed by exposure to 5 or 10 J/cm^2 illumination, respectively. The effect of phototoxicity on cell viability was assessed by CCK-8 assay after 24 h. Data are expressed as the mean ± SD (n = 3). $^bP < 0.01$, $^cP < 0.001$ *vs* the corresponding group without YLG-1 treatment. YLG-1: (17R,18R)-2-(1-hexyloxyethyl)-2-devinyl chlorine E6 trisodium salt; FL: Fluorescence.

to perform YLG-1-PDT was 2 h after IT injection.

Growth inhibition of YLG-1-PDT on pancreatic tumors in vivo

Encouraged by the antitumor effects of YLG-1-PDT *in vitro*, mice in the PDT group were treated with 8 mg/kg YLG-1 by IT injection and exposed to 650 nm laser-irradiation (100 J/cm^2) at 2 h postinjection. Images were taken at 0-14 d post-PDT to show the dynamic changes. Tumors treated with YLG-1-PDT gradually became dark, shrunk within 6 d, and eventually formed a scab by 14 d (Figure 6B). In contrast, tumors in the Con, YLG-1, and Light groups continued to grow, and there were no significant differences among the tumor volumes in the three groups (Figure 6A). The PDT group exhibited significantly smaller tumors than the Con group during the 6-14 d posttreatment. Similarly, tumors weights in the PDT group were significantly lower than those in the Con group at 14 d posttreatment (Figure 6C). Tissues from the Con group displayed pleomorphic cell nuclei, compact tumor cells, and an intact structure. No remarkable morphological differences were observed between the YLG-1, Light, and Con groups. However, cellular swelling, nuclear fragments, and large areas of necrosis were observed in the PDT group (Figure 6D). These data further supported the antitumor effects of YLG-1-PDT on pancreatic neoplasms *in vivo*.

DISCUSSION

Effective treatment regimens remain an urgent need for pancreatic cancer due to its poor prognosis. PDT was demonstrated to inhibit the growth of pancreatic cancer cells in fundamental and clinical experiments[16-19]. Advancements in EUS have made PDT a feasible clinical therapy for pancreatic cancer. The development of appropriate photosensitizers is highly desired to improve the effects of PDT. Here, we demonstrated that YLG-1 had potent PDT effects for use in pancreatic cancer therapy.

The high phototoxic effect of a photosensitizer is an essential feature for PDT. In our study, we found that YLG-1 had a broad safe dose up to at least 5 μg/mL in pancreatic cancer. Due to its high water-solubility, YLG-1 could exert potent phototoxicity in both cells lines at less than 0.5 μg/mL (10 J/cm^2). These data indicated that YLG-1 is a safe and efficient photosensitizer.

It has been widely accepted that PDT-induced cytotoxicity is attributed to the generation of ROS. Here, we detected a significant increase in ROS production at 1 h post-YLG-1-PDT treatment. The crucial role of ROS in YLG-1-PDT was further confirmed using the ROS scavenger NAC, which recovered pancreatic cancer cell viability. Next, we observed the distribution of YLG-1 in the mitochondria and YLG-1-PDT-induced apoptosis in pancreatic cancer cells. Because the subcellular localization of a photosensitizer can impact its mechanisms of action, we considered that the mitochondria-caspase pathway was probably involved in the apoptotic mechanism. It is well known that Bax and cleaved Caspase-3 (active Caspase-3) are pro-apoptotic proteins and Bcl-2 is an antiapoptotic protein[20-23]. As expected, Bax and cleaved Caspase-3 expression was significantly upregulated by YLG-1-PDT, while Bcl-2 expression exhibited the opposite results. Our data suggested that YLG-1-PDT could eradicate pancreatic cancer cells by inducing ROS and promoting apoptosis, accompanied by an increase in Bax and cleaved Caspase-3 expression and a decrease in Bcl-2 expression.

The highly hydrophilic properties of a photosensitizer are a double-edged sword. It can enhance their efficiency locally, but it is always accompanied by their rapid clearance from blood circulation, resulting in lacking tumor-targeting abilities. As we expected, YLG-1 did not exhibit tumor-specific accumulation *via* systemic IP

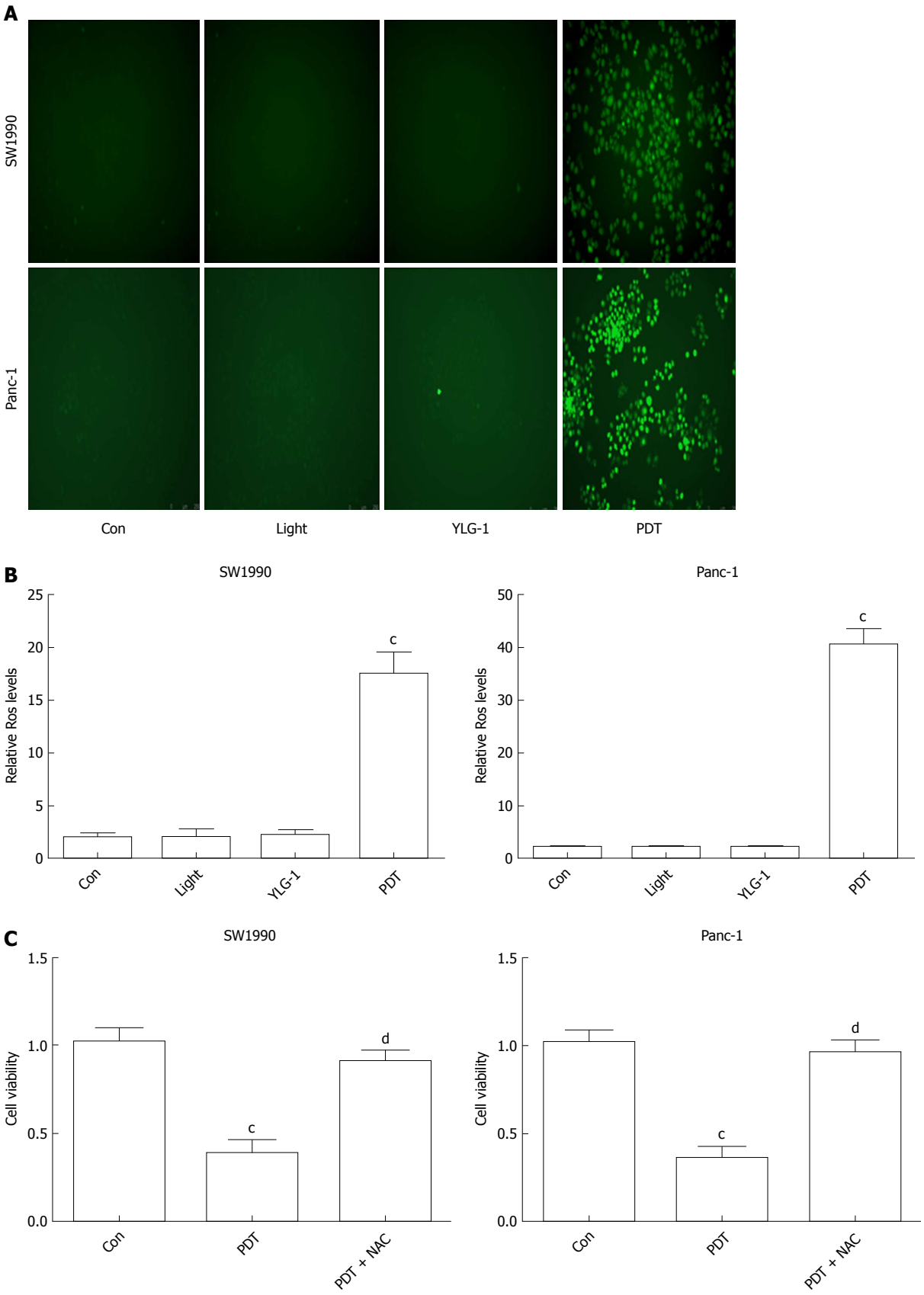

Figure 3 (17R,18R)-2-(1-hexyloxyethyl)-2-devinyl chlorine E6 trisodium salt-induced photodynamic therapy kills pancreatic cancer cells by inducing reactive oxygen species. A: Fluorescence images of intracellular reactive oxygen species (ROS) in SW1990 and Panc-1 cells at 1 h post-photodynamic therapy (PDT) (magnification, 200×). B: Quantitative analysis of ROS production using the scanning multimode reader. C: Effect of the ROS scavenger N-acetyl-L-cysteine on the cytotoxicity induced by (17R,18R)-2-(1-hexyloxyethyl)-2-devinyl chlorine E6 trisodium salt-induced PDT. Data are expressed as the mean ± SD (n = 3). $^{c}P < 0.001$ *vs* Con group, $^{d}P < 0.001$ *vs* the PDT group. FL: Fluorescence; ROS: Reactive oxygen species; YLG-1: (17R,18R)-2-(1-hexyloxyethyl)-2-devinyl chlorine E6 trisodium salt; PDT: Photodynamic therapy; NAC: N-acetyl-L-cysteine.

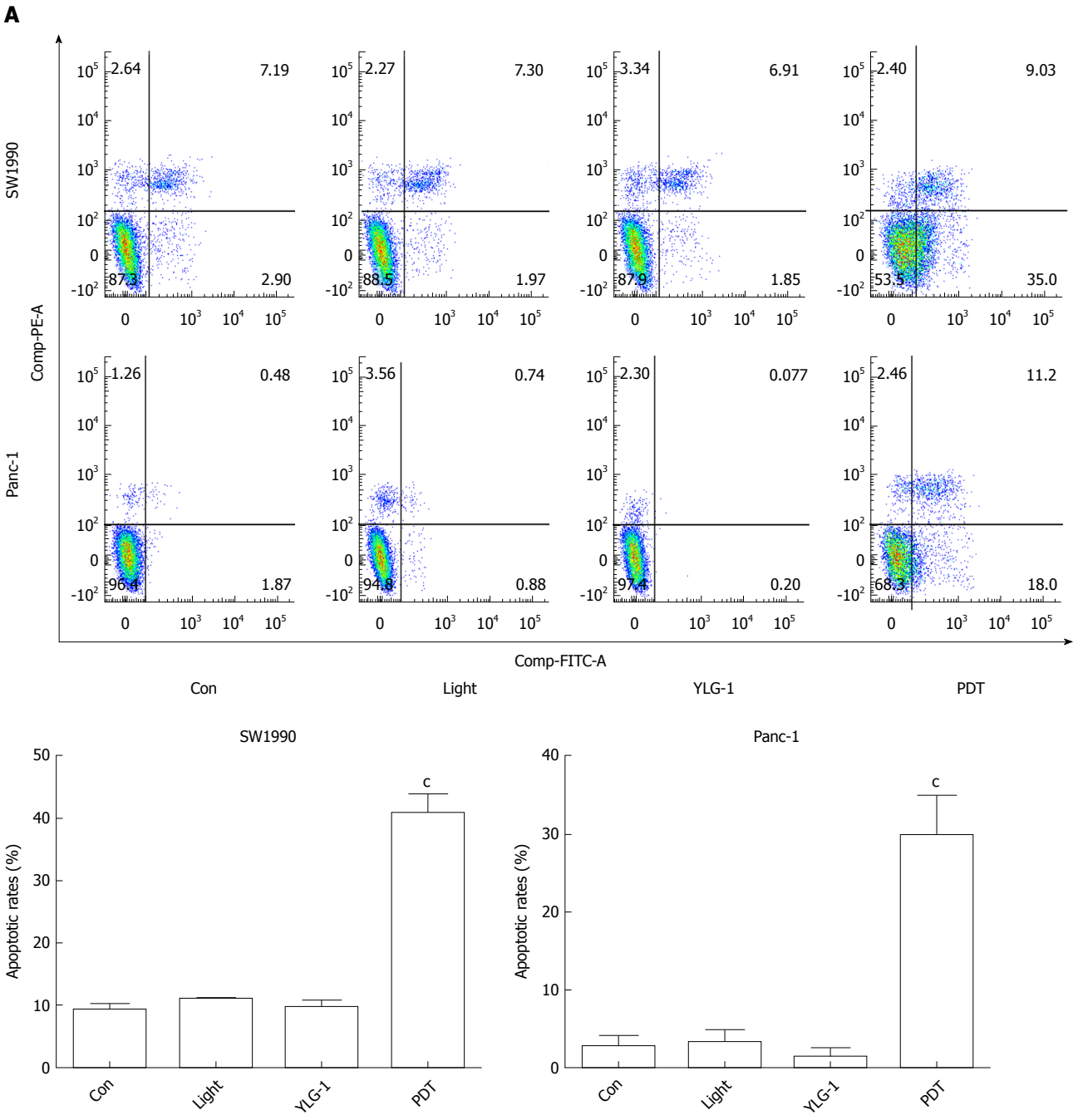
A
SW1990
Panc-1
Comp-PE-A
Comp-FITC-A
2.64
7.19
87.3
2.90
2.27
7.30
88.5
1.97
3.34
6.91
87.9
1.85
2.40
9.03
53.5
35.0
1.26
0.48
96.4
1.87
3.56
0.74
94.8
0.88
2.30
0.077
97.4
0.20
2.46
11.2
68.3
18.0
Con
Light
YLG-1
PDT
SW1990
Panc-1
Apoptotic rates (%)
c
Con
Light
YLG-1
PDT
B
Cleaved Cap3
Bax
Bcl-2
β-actin
SW1990
Panc-1

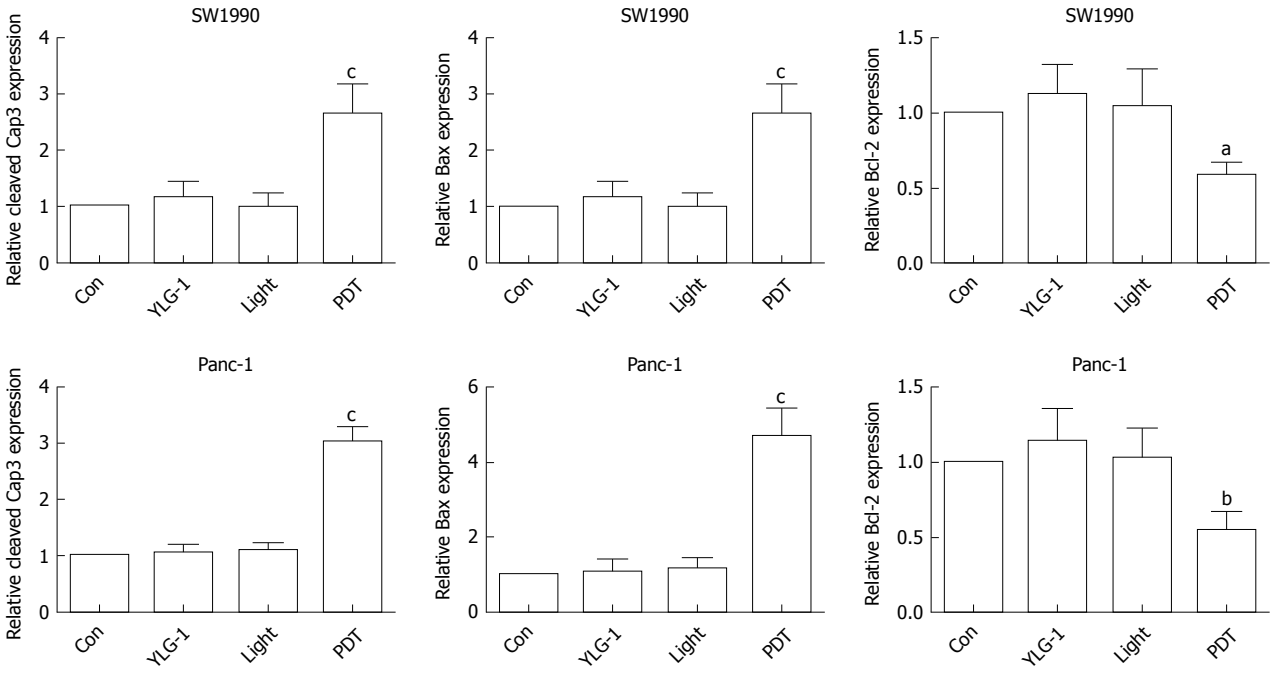

Figure 4 (17R,18R)-2-(1-hexyloxyethyl)-2-devinyl chlorine E6 trisodium salt-induced photodynamic therapy promotes pancreatic cancer cell apoptosis *in vitro*. A: Analysis of apoptosis rate by flow cytometry at 4 h post photodynamic therapy. B: Bcl-2, Bax, and, cleaved Caspase-3 protein levels determined by Western blot. β-actin was used as an internal reference. Data are expressed as the mean ± SD (n = 3). $^{a}P < 0.05$, $^{b}P < 0.01$, and $^{c}P < 0.001$ *vs* the Con group. YLG-1: (17R,18R)-2-(1-hexyloxyethyl)-2-devinyl chlorine E6 trisodium salt; PDT: Photodynamic therapy.

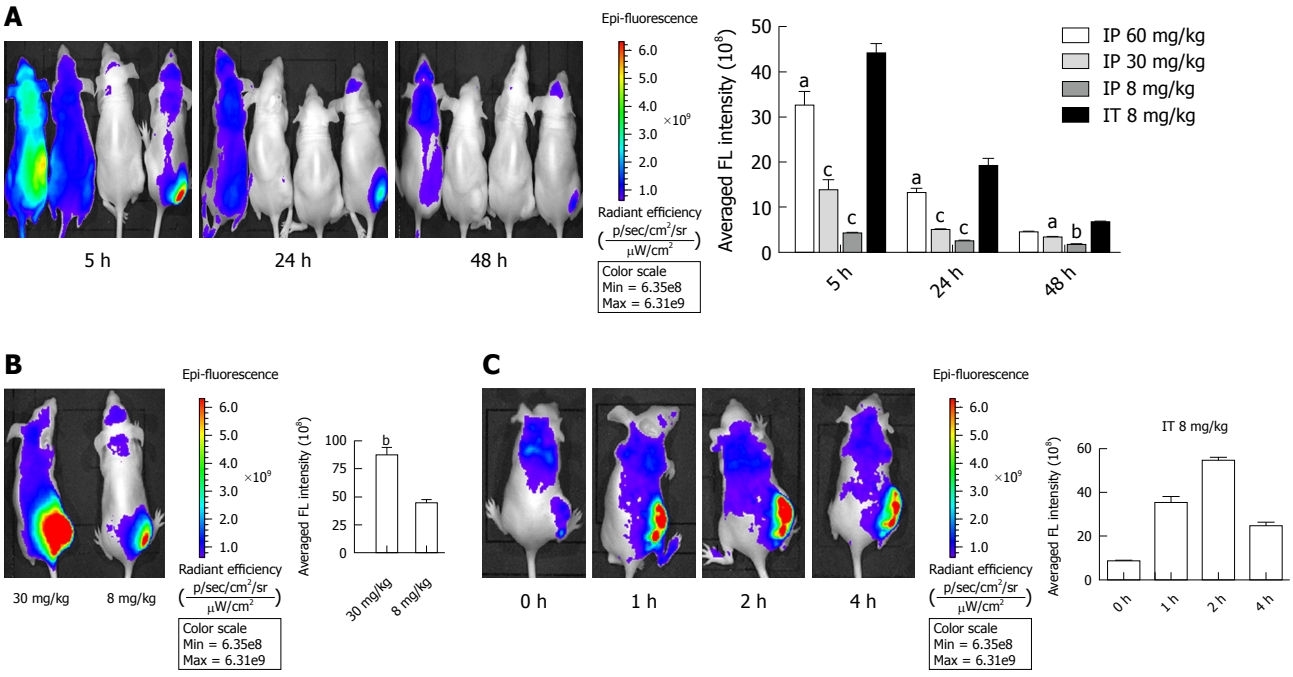

Figure 5 Biodistribution of (17R,18R)-2-(1-hexyloxyethyl)-2-devinyl chlorine E6 trisodium salt *in vivo*. A: *In vivo* fluorescence (FL) images and quantitative evaluation of the Panc-1 tumor-bearing mice at 5, 24, and 48 h post-intraperitoneal (IP) or -intratumoral (IT) injection of (17R,18R)-2-(1-hexyloxyethyl)-2-devinyl chlorine E6 trisodium salt (YLG-1). Mice listed from left to right were respectively administered with 60, 30, and 8 mg/kg YLG-1 *via* IP injection and 8 mg/kg YLG-1 by IT injection. B: *In vivo* FL image and quantitative analysis of mice at 5 h after IT injection with 30 or 8 mg/kg YLG-1. C: *In vivo* FL images and quantitative analysis of mice at 0, 1, 2, and 4 h post-IT injection of 8 mg/kg YLG-1. The FL intensity of YLG-1 in the tumor site was quantified using the same color scale (min = $6.35e^{8}$ and max = $6.31e^{9}$). The data are shown as the mean ± SD (n = 3). $^{a}P < 0.05$, $^{b}P < 0.01$, and $^{c}P < 0.001$ *vs* the corresponding IT injection group. YLG-1: (17R,18R)-2-(1-hexyloxyethyl)-2-devinyl chlorine E6 trisodium salt; FL: Fluorescence; IP: Intraperitoneal; IT: Intratumoral.

injection (even up to 60 mg/kg). For photosensitizers with high water solubility, IT injection might be an appropriate way to promote their accumulation in tumor tissues. Administration *via* IT injection with only 8 mg/kg YLG-1 could achieve a strong and long-term FL intensity within the tumor area. This suggested that the

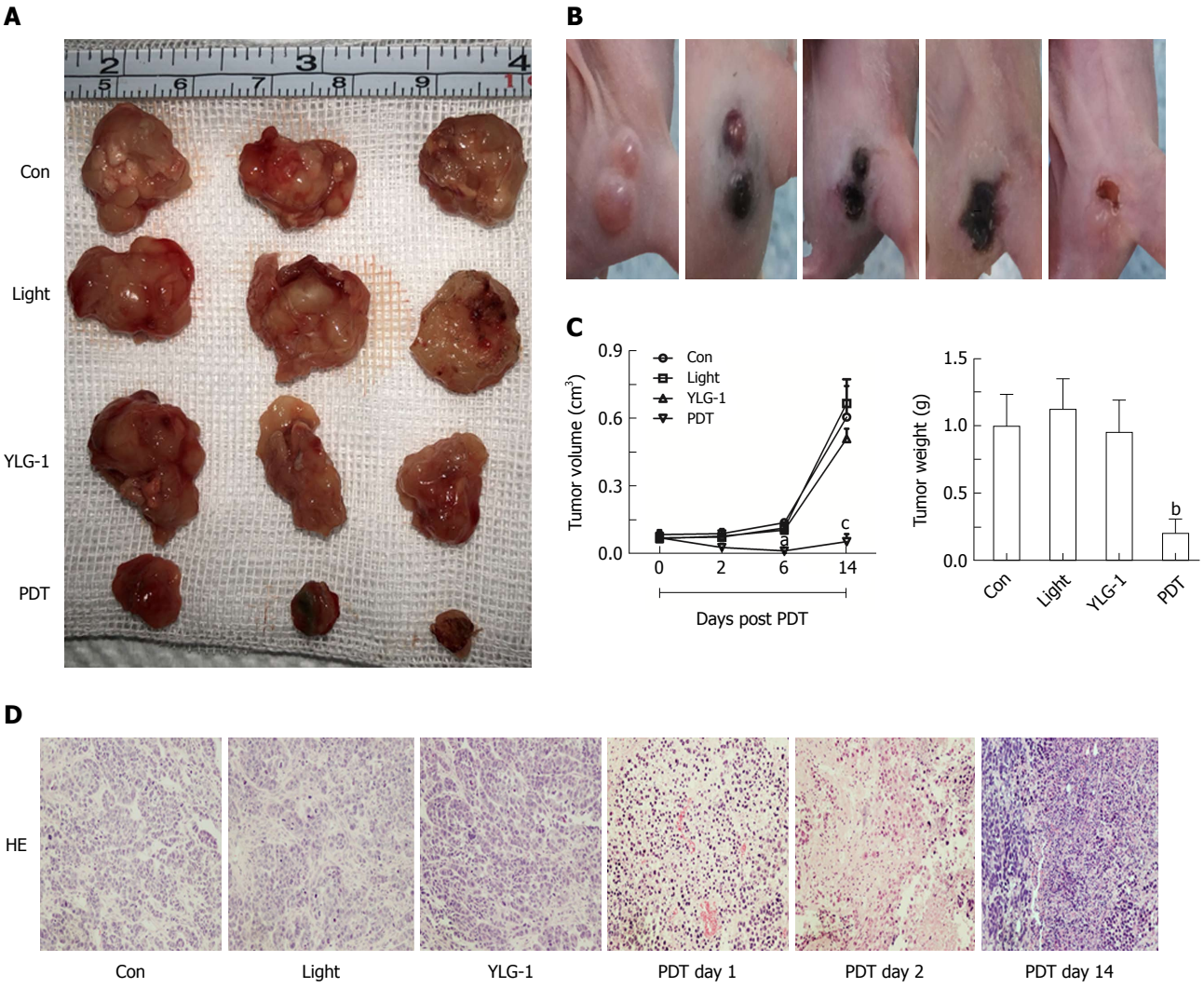

Figure 6 (17R,18R)-2-(1-hexyloxyethyl)-2-devinyl chlorine E6 trisodium salt-induced photodynamic therapy inhibits the growth of pancreatic carcinoma *in vivo*. A: Images of Panc-1 tumors at 14 d post-photodynamic therapy (PDT) [8 mg/kg (17R,18R)-2-(1-hexyloxyethyl)-2-devinyl chlorine E6 trisodium salt (YLG-1), intratumoral (IT) injection] with or without 100 J/cm^2 illumination. B: The dynamic changes in pancreatic cancers treated by YLG-1-PDT over 14 d. C: Tumor volumes and weights at the indicated time. D: The hematoxylin and eosin staining of tumor sections acquired at 1, 2, and, 14 d post-PDT. Images were captured under a light microscope (magnification, 200×). The results are expressed as the mean ± SD (n = 3). $^aP < 0.05$, $^bP < 0.01$, and $^cP < 0.001$ *vs* the Con group at the indicated time. YLG: (17R,18R)-2-(1-hexyloxyethyl)-2-devinyl chlorine E6 trisodium salt; PDT: Photodynamic therapy; IT: Intratumoral.

optimal administration route for YLG-1 was IT injection. Indeed, IT injection is an acknowledged administration route applied in many studies[24-27]. Compared with conventional systematic administration, a small amount of photosensitizer could be effective *via* IT injection. We believe that IT injection should be attempted to apply clinical PDT, especially for hypovascular tumors such as pancreatic cancer. Inspired by the direct insertion of an EUS-mediated laser-light catheter into tumors to deliver sufficient illumination in pancreatic cancer PDT[8], we proposed that an EUS-guided IT injection method with a photosensitizer using a puncture needle might be a feasible and appropriate way for photosensitizer accumulation in pancreatic tumor tissue. Based on our experiments, we believe that YLG-1 might be suitable for superficial, luminal, and hypovascular tumors that require topical administration, and that YLG-1 might be a promising photosensitizer in pancreatic cancer PDT.

Aside from changing the drug delivery route, modifying YLG-1 is another solution to improve the concentration of photosensitizer in tumors. Hu *et al*[28] developed nanoparticles by hierarchically assembling doxorubicin (DOX), Ce6, and colloidal manganese dioxide (MnO2) with poly (ε-caprolactone-co-lactide)-b-poly (ethylene glycol)-b-poly (ε-caprolactone-co-lactide) to treat breast cancer, which enhanced tumor uptake of the photosensitizer by prolonging its blood circulation. We wonder whether YLG-1 has the potential to be modified in that way; thus, more research focused on YLG-1 characteristics should be performed in the future.

We next demonstrated that YLG-1-PDT significantly decreased the growth of pancreatic tumors *in vivo* by IT administration. The tumors treated with PDT mostly disappeared at 6 d posttreatment and were significantly smaller than the untreated group during the 6-14 d. However, at 14 d posttreatment, the tumors returned,

though with much smaller tumor volumes. Therefore, similar to other anticancer therapies, PDT could leave behind a significant number of surviving tumor cells, as cancer cells surrounding the focally treated area were always subjected to a low dose laser light. The surviving cells are likely to become the source for relapse and metastasis. This suggested that multipoint fiber insertion irradiation or multiple PDT or multimodal regimens were indispensable for clinical pancreatic neoplasm PDT.

In conclusion, our results demonstrate that YLG-1-PDT has a potent antitumor effect on pancreatic cancer cells *via* inducing ROS and apoptosis. Although YLG-1 lacks specific tumor-targeting accumulation due to its small and highly soluble nature, it could contribute to locally high efficiency *via* topical delivery. With regard to the hypovascular characteristics of pancreatic tumors, IT injection, rather than systemic administration, is the appropriate drug delivery route. Hence, we assume that YLG-1 is a potential photosensitizer for pancreatic neoplasm PDT. To apply YLG-1 in more cancers, further studies should focus on modifying YLG-1 to target tumor accumulation.

ARTICLE HIGHLIGHTS

Research background

With the development of endoscopic ultrasonography (EUS) and EUS-guided fine needle aspiration (EUS-FNA), photodynamic therapy (PDT) has become a feasible treatment for advanced pancreatic neoplasms. The selection of an appropriate photosensitizer is of great importance in PDT. (17R,18R)-2-(1-hexyloxyethyl)-2-devinyl chlorine E6 trisodium salt (YLG-1) is hydrophilic chlorine derivative extracted from spirulina. It possesses characteristics including high purity, high water-solubility, high chemical stability, high phototoxicity, low dark toxicity as well as low price. Initially, YLG-1 was approved as a disinfection product for its great antimicrobial effect under illumination. However, the functions of YLG-1 in PDT are still poorly understood with no available publication.

Research motivation

Our findings will provide fundamental research for the clinical application of YLG-1 in pancreatic cancer therapy.

Research objectives

To explore the antitumor effects of YLG-1-induced PDT (YLG-1-PDT) on pancreatic cancer cells and its underlying mechanisms in vitro and in vivo.

Research methods

The human pancreatic cancer cell lines SW1990 and Panc-1 were used to detect the effects of YLG-1. CCK-8 assay, Bio-Tek Synergy H1, confocal microscopy, DCFH-DA, flow cytometry, and Western blot were exploited to detected the phototoxicity, cellular uptake, localization, reactive oxygen species (ROS) production, apoptosis and apoptosis-associated proteins (Bax, Bcl-2, and cleaved Caspase-3) expression, respectively. An *in vivo* imaging system (IVIS), the Lumina K imaging system, and mouse models of subcutaneous Panc-1-bearing tumors were used to assess the drug-delivered way of YLG-1 and pancreatic tumor growth *in vivo*.

Research results

YLG-1 was located in mitochondria and the appropriated incubation time was 6 h. Under 650 nm illumination, YLG-1 exhibited a potent phototoxicity on pancreatic cancer cells with a great generation of ROS *in vitro*. Besides, YLG-1-PDT induced pancreatic cancer cell apoptosis, upregulated Bax and cleaved Caspase-3 expression and decreased Bcl-2 expression. IVIS images indicated the optimal administration of YLG-1 was intratumoral (IT) injection and the best time to perform PDT was 2 h post IT injection. In accordance with the results *in vitro*, YLG-1-PDT potently inhibited the growth of pancreatic cancer cells in a mouse model. Notably, due to its small and highly soluble nature, YLG-1 lacked specific tumor-targeting accumulation and had better be applied by topical administration.

Research conclusions

YLG-1 is a potential photosensitizer for pancreatic cancer PDT *via* IT injection, the mechanisms of which are related with inducing ROS and promoting apoptosis. Hence, YLG-1-PDT might be a promising component of multimodality therapy of pancreatic neoplasms.

Research perspectives

Our results demonstrated that YLG-1-PDT had a potent antitumor effect on pancreatic cancer cells *via* inducing ROS and apoptosis. Since YLG-1 is lack of specific tumor-targeting accumulation, it might be suitable for superficial, luminal, and hypovascular tumors that need topical administration. Thus, YLG-1 is a promising photosensitizer in pancreatic cancer PDT in terms of its hypovascular character. In order to apply YLG-1 in more cancers, further studies should focus on modifying YLG-1 for target tumor accumulation.

REFERENCES

1 **Kamisawa T**, Wood LD, Itoi T, Takaori K. Pancreatic cancer. *Lancet* 2016; **388**: 73-85 [PMID: 26830752 DOI: 10.1016/S0140-6736(16)00141-0]

2 **Kleeff J**, Korc M, Apte M, La Vecchia C, Johnson CD, Biankin AV, Neale RE, Tempero M, Tuveson DA, Hruban RH, Neoptolemos JP. Pancreatic cancer. *Nat Rev Dis Primers* 2016; **2**: 16022 [PMID: 27158978 DOI: 10.1038/nrdp.2016.22]

3 **Mallidi S**, Anbil S, Bulin AL, Obaid G, Ichikawa M, Hasan T. Beyond the Barriers of Light Penetration: Strategies, Perspectives and Possibilities for Photodynamic Therapy. *Theranostics* 2016; **6**: 2458-2487 [PMID: 27877247 DOI: 10.7150/thno.16183]

4 **Cieplik F**, Deng D, Crielaard W, Buchalla W, Hellwig E, Al-Ahmad A, Maisch T. Antimicrobial photodynamic therapy - what we know and what we don't. *Crit Rev Microbiol* 2018; **44**: 571-589 [PMID: 29749263 DOI: 10.1080/1040841X.2018.1467876]

5 **Kwiatkowski S**, Knap B, Przystupski D, Saczko J, Kędzierska E, Knap-Czop K, Kotlińska J, Michel O, Kotowski K, Kulbacka J. Photodynamic therapy - mechanisms, photosensitizers and combinations. *Biomed Pharmacother* 2018; **106**: 1098-1107 [PMID: 30119176 DOI: 10.1016/j.biopha.2018.07.049]

6 **Yang Y**, Hu Y, Wang H. Targeting Antitumor Immune Response for Enhancing the Efficacy of Photodynamic Therapy of Cancer: Recent Advances and Future Perspectives. *Oxid Med Cell Longev* 2016; **2016**: 5274084 [PMID: 27672421 DOI: 10.1155/2016/5274084]

7 **van Straten D**, Mashayekhi V, de Bruijn HS, Oliveira S, Robinson DJ. Oncologic Photodynamic Therapy: Basic Principles, Current Clinical Status and Future Directions. *Cancers* (Basel) 2017; **9**: [PMID: 28218708 DOI: 10.3390/cancers9020019]

8 **Choi JH**, Oh D, Lee JH, Park JH, Kim KP, Lee SS, Lee YJ, Lim YS, Song TJ, Lee SS, Seo DW, Lee SK, Kim MH, Park DH. Initial human experience of endoscopic ultrasound-guided photodynamic therapy with a novel photosensitizer and a flexible laser-light catheter. *Endoscopy* 2015; **47**: 1035-1038 [PMID: 26070006 DOI: 10.1055/s-0034-1392150]

9 **Usuda J**, Ichinose S, Ishizumi T, Hayashi H, Ohtani K, Maehara S, Ono S, Honda H, Kajiwara N, Uchida O, Tsutsui H, Ohira T, Kato H, Ikeda N. Outcome of photodynamic therapy using NPe6 for bronchogenic carcinomas in central airways >1.0 cm in diameter. *Clin Cancer Res* 2010; **16**: 2198-2204 [PMID: 20332318 DOI: 10.1158/1078-0432.CCR-09-2520]

10 **Chang JE**, Liu Y, Lee TH, Lee WK, Yoon I, Kim K. Tumor Size-Dependent Anticancer Efficacy of Chlorin Derivatives for Photodynamic Therapy. *Int J Mol Sci* 2018; **19** [PMID: 29844257 DOI: 10.3390/ijms19061596]

11 **Zeinalian R**, Farhangi MA, Shariat A, Saghafi-Asl M. The effects of

Spirulina Platensis on anthropometric indices, appetite, lipid profile and serum vascular endothelial growth factor (VEGF) in obese individuals: a randomized double blinded placebo controlled trial. *BMC Complement Altern Med* 2017; **17**: 225 [PMID: 28431534 DOI: 10.1186/s12906-017-1670-y]

12 **Jeon YM**, Lee HS, Jeong D, Oh HK, Ra KH, Lee MY. Antimicrobial photodynamic therapy using chlorin e6 with halogen light for acne bacteria-induced inflammation. *Life Sci* 2015; **124**: 56-63 [PMID: 25623849 DOI: 10.1016/j.lfs.2014.12.029]

13 **Liu Z**, Fu X, Huang W, Li C, Wang X, Huang B. Photodynamic effect and mechanism study of selenium-enriched phycocyanin from Spirulina platensis against liver tumours. *J Photochem Photobiol B* 2018; **180**: 89-97 [PMID: 29413706 DOI: 10.1016/j.jphotobiol.2017.12.020]

14 **Srivatsan A**, Pera P, Joshi P, Wang Y, Missert JR, Tracy EC, Tabaczynski WA, Yao R, Sajjad M, Baumann H, Pandey RK. Effect of chirality on cellular uptake, imaging and photodynamic therapy of photosensitizers derived from chlorophyll-a. *Bioorg Med Chem* 2015; **23**: 3603-3617 [PMID: 25936263 DOI: 10.1016/j.bmc.2015.04.006]

15 **Chen WH**, Lecaros RL, Tseng YC, Huang L, Hsu YC. Nanoparticle delivery of HIF1α siRNA combined with photodynamic therapy as a potential treatment strategy for head-and-neck cancer. *Cancer Lett* 2015; **359**: 65-74 [PMID: 25596376 DOI: 10.1016/j.canlet.2014.12.052]

16 **Ding F**, Li HJ, Wang JX, Tao W, Zhu YH, Yu Y, Yang XZ. Chlorin e6-Encapsulated Polyphosphoester Based Nanocarriers with Viscous Flow Core for Effective Treatment of Pancreatic Cancer. *ACS Appl Mater Interfaces* 2015; **7**: 18856-18865 [PMID: 26267601 DOI: 10.1021/acsami.5b05724]

17 **Huggett MT**, Jermyn M, Gillams A, Illing R, Mosse S, Novelli M, Kent E, Bown SG, Hasan T, Pogue BW, Pereira SP. Phase I/II study of verteporfin photodynamic therapy in locally advanced pancreatic cancer. *Br J Cancer* 2014; **110**: 1698-1704 [PMID: 24569464 DOI: 10.1038/bjc.2014.95]

18 **Roh YJ**, Kim JH, Kim IW, Na K, Park JM, Choi MG. Photodynamic Therapy Using Photosensitizer-Encapsulated Polymeric Nanoparticle to Overcome ATP-Binding Cassette Transporter Subfamily G2 Function in Pancreatic Cancer. *Mol Cancer Ther* 2017; **16**: 1487-1496 [PMID: 28416605 DOI: 10.1158/1535-7163.MCT-16-0642]

19 **Li MM**, Cao J, Yang JC, Shen YJ, Cai XL, Chen YW, Qu CY, Zhang Y, Shen F, Xu LM. Effects of arginine-glycine-aspartic acid peptide-conjugated quantum dots-induced photodynamic therapy on pancreatic carcinoma in vivo. *Int J Nanomedicine* 2017; **12**: 2769-2779 [PMID: 28435257 DOI: 10.2147/IJN.S130799]

20 **Li KT**, Chen Q, Wang DW, Duan QQ, Tian S, He JW, Ou YS, Bai DQ. Mitochondrial pathway and endoplasmic reticulum stress participate in the photosensitizing effectiveness of AE-PDT in MG63 cells. *Cancer Med* 2016; **5**: 3186-3193 [PMID: 27700017 DOI: 10.1002/cam4.895]

21 **Shao J**, Xue J, Dai Y, Liu H, Chen N, Jia L, Huang J. Inhibition of human hepatocellular carcinoma HepG2 by phthalocyanine photosensitiser PHOTOCYANINE: ROS production, apoptosis, cell cycle arrest. *Eur J Cancer* 2012; **48**: 2086-2096 [PMID: 22265427 DOI: 10.1016/j.ejca.2011.10.013]

22 **Liu YQ**, Meng PS, Zhang HC, Liu X, Wang MX, Cao WW, Hu Z, Zhang ZG. Inhibitory effect of aloe emodin mediated photodynamic therapy on human oral mucosa carcinoma in vitro and in vivo. *Biomed Pharmacother* 2018; **97**: 697-707 [PMID: 29102913 DOI: 10.1016/j.biopha.2017.10.080]

23 **Allison RR**, Moghissi K. Photodynamic Therapy (PDT): PDT Mechanisms. *Clin Endosc* 2013; **46**: 24-29 [PMID: 23422955 DOI: 10.5946/ce.2013.46.1.24]

24 **Foster TH**, Giesselman BR, Hu R, Kenney ME, Mitra S. Intratumor administration of the photosensitizer pc 4 affords photodynamic therapy efficacy and selectivity at short drug-light intervals. *Transl Oncol* 2010; **3**: 135-141 [PMID: 20360938 DOI: 10.1593/tlo.09295]

25 **Ai F**, Wang N, Zhang X, Sun T, Zhu Q, Kong W, Wang F, Zhu G. An upconversion nanoplatform with extracellular pH-driven tumor-targeting ability for improved photodynamic therapy. *Nanoscale* 2018; **10**: 4432-4441 [PMID: 29451577 DOI: 10.1039/c7nr06874c]

26 **Luo Z**, Zheng M, Zhao P, Chen Z, Siu F, Gong P, Gao G, Sheng Z, Zheng C, Ma Y, Cai L. Self-Monitoring Artificial Red Cells with Sufficient Oxygen Supply for Enhanced Photodynamic Therapy. *Sci Rep* 2016; **6**: 23393 [PMID: 26987618 DOI: 10.1038/srep23393]

27 **Dou X**, Nomoto T, Takemoto H, Matsui M, Tomoda K, Nishiyama N. Effect of multiple cyclic RGD peptides on tumor accumulation and intratumoral distribution of IRDye 700DX-conjugated polymers. *Sci Rep* 2018; **8**: 8126 [PMID: 29802410 DOI: 10.1038/s41598-018-26593-0]

28 **Hu D**, Chen L, Qu Y, Peng J, Chu B, Shi K, Hao Y, Zhong L, Wang M, Qian Z. Oxygen-generating Hybrid Polymeric Nanoparticles with Encapsulated Doxorubicin and Chlorin e6 for Trimodal Imaging-Guided Combined Chemo-Photodynamic Therapy. *Theranostics* 2018; **8**: 1558-1574 [PMID: 29556341 DOI: 10.7150/thno.22989]

P- Reviewer: Ashida R, Guo XZ **S- Editor**: Ma RY
L- Editor: Wang TQ **E- Editor**: Yin SY

Published by **Baishideng Publishing Group Inc**
7901 Stoneridge Drive, Suite 501, Pleasanton, CA 94588, USA
Telephone: +1-925-223-8242
Fax: +1-925-223-8243
E-mail: bpgoffice@wjgnet.com
Help Desk: https://www.f6publishing.com/helpdesk
https://www.wjgnet.com

ISSN 1007-9327
9 771007 932045 46>